Ship localization in Santa Barbara Channel using machine learning classifiers

Haiqiang Niu,[a] **Emma Ozanich, and Peter Gerstoft**
Scripps Institution of Oceanography, University of California San Diego, La Jolla, California 92093-0238, USA
hniu@ucsd.edu, ecreeves@ucsd.edu, pgerstoft@ucsd.edu

Abstract: Machine learning classifiers are shown to outperform conventional matched field processing for a deep water (600 m depth) ocean acoustic-based ship range estimation problem in the Santa Barbara Channel Experiment when limited environmental information is known. Recordings of three different ships of opportunity on a vertical array were used as training and test data for the feed-forward neural network and support vector machine classifiers, demonstrating the feasibility of machine learning methods to locate unseen sources. The classifiers perform well up to 10 km range whereas the conventional matched field processing fails at about 4 km range without accurate environmental information.

[PEB]
Date Received: July 31, 2017 **Date Accepted:** October 21, 2017

1. Introduction

Recently, a single ship was localized in a shallow water environment (water depth 152 m) using machine learning methods that learn a propagation relationship from the received acoustic pressure on a vertical array and the known ship GPS.[1] The feed-forward neural network (FNN), support vector machine (SVM), and random forest (RF) methods achieved similar results but performed best when posed as a classification problem with data at a wide range of frequencies. In general, the model-free machine learning methods achieved lower error than conventional matched field processing (MFP). This study solves the ship localization problem in the deep water environment of the Santa Barbara Channel (water depth 540–600 m). The FNN and SVM classifiers are trained and tested using three different sources of opportunity (transiting ships) with varying speeds.

Unlike matched field processing (MFP)[2,3] approaches, machine learning methods learn directly from the data, allowing them to overcome some challenges of environmental mismatch in modeling. Machine learning in ocean acoustics was conducted using theory and computational resources in the 1990s.[4–9] A recent example of machine learning in ocean acoustics is the application of nonlinear regression[10] to source localization. In addition, data-driven linear cross correlation methods were used to localize sources of opportunity in shallow[11,12] and deep[13] water. Here, we focus on data-driven ocean acoustic applications using nonlinear machine learning tools.

2. Localization based on machine learning

The localization problem is solved as follows:[1]

(1) Preprocess input data. The recorded pressure data are formed into the sample covariance matrices (SCMs) and then vectorized to generate the input data of the classifiers.
(2) Divide the preprocessed data into training and test data sets. The labels are designed for the training data using known GPS locations.
(3) Train the classifier models on the training data set.
(4) Predict the source ranges on test data set using the trained model parameters.

2.1 Input data preprocessing

The received array data is preprocessed to minimize the effect of the complex source spectra. Following Ref. 1, the complex pressure $\mathbf{p}(f)$ at frequency f is normalized by

[a]Author to whom correspondence should be addressed. Also at: State Key Laboratory of Acoustics, Institute of Acoustics, Chinese Academy of Sciences, Beijing 100190, People's Republic of China.

$$\tilde{\mathbf{p}}(f) = \frac{\mathbf{p}(f)}{\|\mathbf{p}(f)\|_2}. \quad (1)$$

The normalized sample covariance matrix (SCM), $\mathbf{C}(f)$, is formed from the normalized sound pressure $\tilde{\mathbf{p}}_s(f)$ at the sth snapshot, and averaged over N_s snapshots,

$$\mathbf{C}(f) = \frac{1}{N_s}\sum_{s=1}^{N_s} \tilde{\mathbf{p}}_s(f)\tilde{\mathbf{p}}_s^H(f). \quad (2)$$

H denotes conjugate transpose operator. $\mathbf{C}(f)$ is a conjugate symmetric matrix. The complex upper triangular matrix entries are separated into the real and imaginary parts and vectorized to form the real-valued input $\mathbf{x}$ of size $L \times (L+1)$ for L sensors.

The objective of the SCM normalization is to remove effects of the source spectrum and allow for training and test data from different sources.[1]

2.2 Labels and structure of classifiers

For the classification problem, a set of source ranges are discretized into K bins, $r_1,\ldots,r_K$, of equal width Δr. Each input vector, $\mathbf{x}_n, n = 1, \ldots, N$, is labeled by t_n, where $t_n \in r_k, k = 1, ..., K$ represents the true source range class. The labels t_n are binary encoded to construct the $N \times K$ target matrix with binary row vectors.

For the FNN, the sigmoid and softmax functions are applied to the hidden and output layer activations. A dropout layer[14] is added before the output layer to reduce overfitting. The cross entropy between the true and predicted labels is used as the cost function. The feed-forward neural network is implemented using TENSORFLOW software[15] with the Adam[16] optimization method with keep probability for training dropout, initial learning rate, and maximum iteration steps of 0.5, 0.001, and 500. The neural network has one hidden layer with 2048 neurons.

For the SVM, a linear kernel function is used here with the regularization parameter $C = 1.0$. The linear kernel function is robust to parameter choice as opposed to the radial basis function and was shown to perform well in this case. The SVM classifier is implemented using the SCIKIT-LEARN package.[17]

More details on the structure of FNN and SVM can be found in Ref. 1.

2.3 Localization accuracy

The mean absolute percentage error (MAPE) is used to quantify the prediction performance of the algorithm,

$$E_{\text{MAPE}} = \frac{100}{N}\sum_{i=1}^{N}\left|\frac{Rp_i - Rg_i}{Rg_i}\right|, \quad (3)$$

where Rp_i and Rg_i are the ith predicted range and the ground truth AIS range, respectively. N is the number of samples.

3. Sea experimental results

3.1 Experimental environment and transmission loss simulation

The Santa Barbara Channel Experiment (SBCEx16) recorded underwater noise from ships exiting or entering Los Angels harbor between 7 and 20 September 2016, see Fig. 1(a). Ships transiting in one of two well-defined shipping lanes were used as the primary acoustic sources in our study. The water depth within this area is 540–600 m.

The experiment geometry of the operation area is shown in Fig. 1(b), with four bottom-moored vertical linear arrays (VLAs) indicated by triangles. The hydrophone sampling rate was 25 kHz. VLA4 is used for range estimation and consists of 28 working hydrophones (77 m aperture spanning 507–584 m depth).

Three ship tracks, recorded during different periods on different ships, were used to form training and test data sets, see Fig. 1(b). All the ships were transiting toward the northwest. The details of these tracks are shown in Table 1. The GPS ship locations used for training labels and ground truth were obtained from the AIS (Automatic Identification System) database.

To examine how SNR decreases with ship range, the transmission loss is simulated with KRAKEN[18] using a range-independent waveguide model. The range-independent waveguide model was chosen to demonstrate the typical limited environmental information available. The source depth is 8 m in a 590 m waveguide with a fluid halfspace bottom (sound speed 1600 m/s, density 1.6 g/cm^3, and attenuation coefficient 0.1 dB/λ). The sound speed profile is from a CTD near VLA4, see Fig. 1(c). The modeled transmission loss at 150 and 300 Hz are typical of deep-water propagation

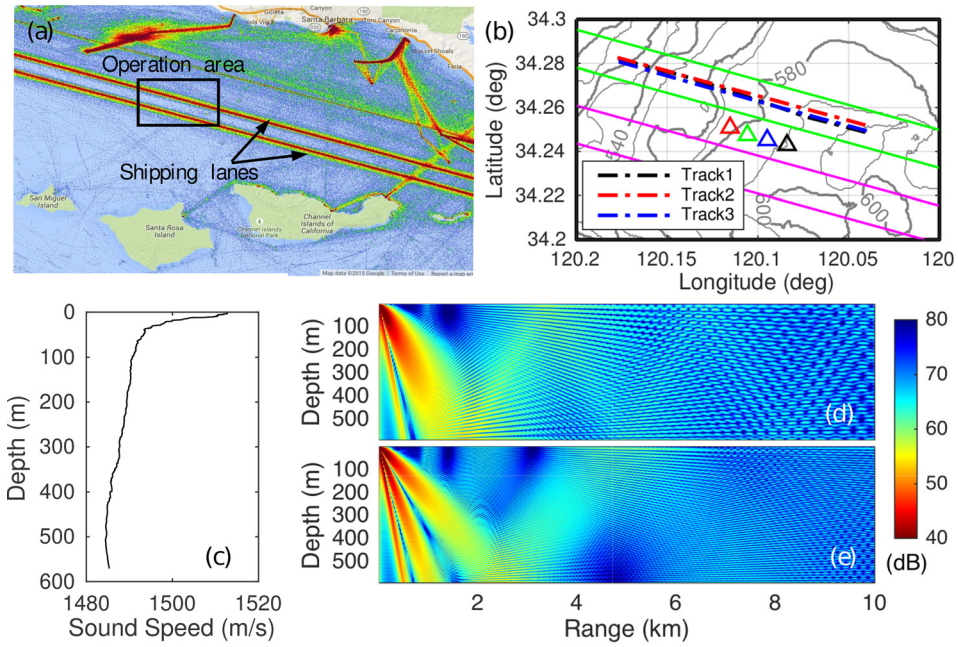

Fig. 1. (Color online) (a) Operation area and two shipping lanes in Santa Barbara Basin. (b) Experiment geometry with three cargo ships transiting operation area. The VLAs are denoted by triangles. (c) Sound speed profile measured by CTD. Transmission loss calculated by KRAKEN at (d) 150 Hz and (e) 300 Hz.

with bottom interaction, see Figs. 1(d) and 1(e). At the receiver depths between 507 and 584 m, the transmission loss increases significantly (from 55 to 70 dB) between the source-receiver ranges of 2 to 10 km with a null (80 dB) for 300 Hz at 5 km range.

The spectrograms of shipping noise recorded on the top hydrophone during the three periods are shown in Fig. 2. The tonal signals (vertical lines) are from the electrical noise of the recording system. The striations in the shipping noise indicate that the ships were moving with different speeds. As seen in Fig. 2, the SNR decreases with increasing source-receiver distance. Two frequency bands are investigated: 53–200 Hz and 203–350 Hz with 3 Hz increment. The first singular value of a 56-snapshot SCM is used to estimate SNR at each frequency at the farthest range (about 10 km). For the three ships, the SNR-range is 5–10, 5–9, 5–8 dB for 53–200 Hz and 3–6, 4–8, 3–6 dB for 203–350 Hz.

3.2 Localization results

Data from Track1 are used as the training data set. Track2 and Track3 are used to form the test data sets Test-Data-1 and Test-Data-2 (Table 1). For each data set, the vectorized SCM at each range and frequency, averaged over five successive 1-s snapshots (four snapshots overlapped), is used as input. There are 1956 samples in the training data set, 260 samples in Test-Data-1, and 300 samples in Test-Data-2. For the training data, the source-receiver ranges are divided into $K = 164$ range bin outputs (50 m increment varying between 1600 and 9750 m).

Multi-frequency SCMs are formed by concatenating multiple single-frequency inputs along the first dimension. The number of input neurons for the multi-frequency case becomes $D = 812 \times N_f$, where N_f is the number of frequencies. In our study, $N_f = 50$ for each of two frequency bands investigated: $f = 53$–200 Hz and $f = 203$–350 Hz with 3 Hz increments.

A comparison of the range predictions on the two test data sets using the Bartlett MFP, SVM, and FNN classifiers is shown in Fig. 3 (53–200 Hz) and Fig. 4 (203–350 Hz) along with R_g (AIS ranges). For the lower frequency band, the MFP,

Table 1. Ship tracks.

Track No.	Data set	Time period	Ship name	Speed (m/s)
Track1	Training-Data	13:00–13:33 (9/15)	KUMANO MARU	6.7
Track2	Test-Data-1	19:11–19:33 (9/16)	APL PHILIPPINES	10
Track3	Test-Data-2	19:29–19:54 (9/17)	NORDSPRING	8.0

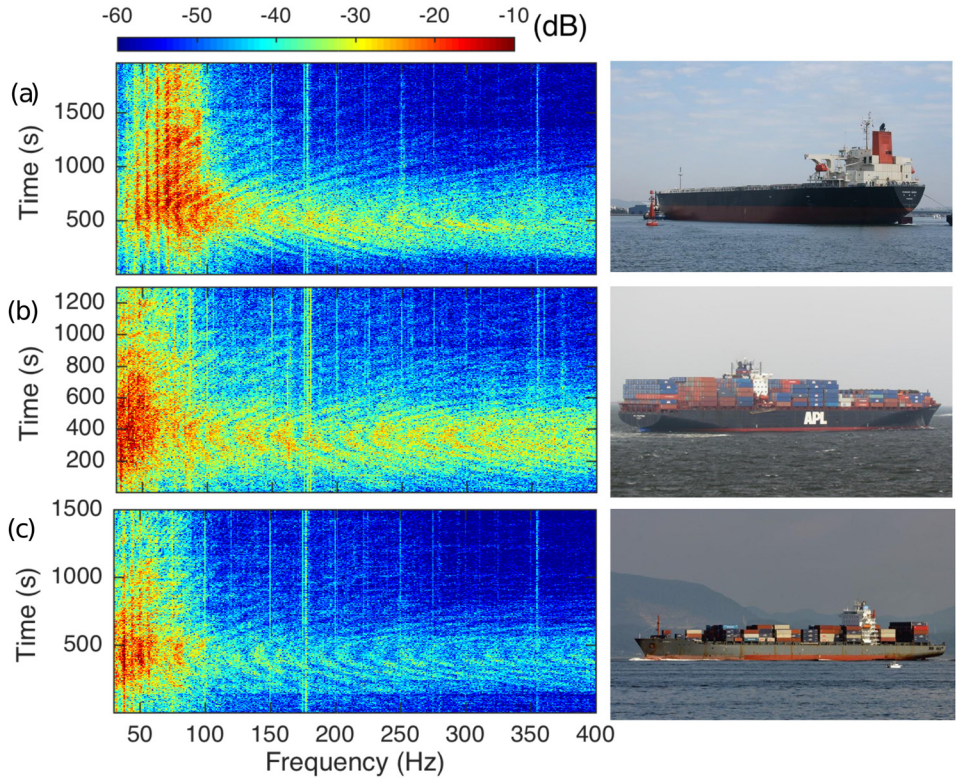

Fig. 2. (Color online) Spectrograms of shipping noise at the top hydrophone during periods (a) September 15, 13:00–13:33, (b) September 16, 19:11–19:33, and (c) September 17, 19:29–19:54. The right column shows the actual appearance of the three ships (photos are from Ref. 19).

SVM, and FNN have a MAPE of 34.6%, 1.5%, and 2.2% on Test-Data-1 and 36.1%, 2.2%, and 3.9% on Test-Data-2. Due to the low SNR and sidelobes, the MFP generates incorrect predictions when the source-receiver range is greater than 4 km. The SVM and FNN classifiers perform well over all the ranges and are robust to low SNR at ranges greater than 4 km.

A similar result is obtained for 203–350 Hz (Fig. 4), with MAPE values of 26.4%, 4.0%, and 7.0% on Test-Data-1 and 49.9%, 4.6%, and 6.3% on Test-Data-2. The SVM and FNN classifiers perform better at 53–200 Hz due to the higher SNR.

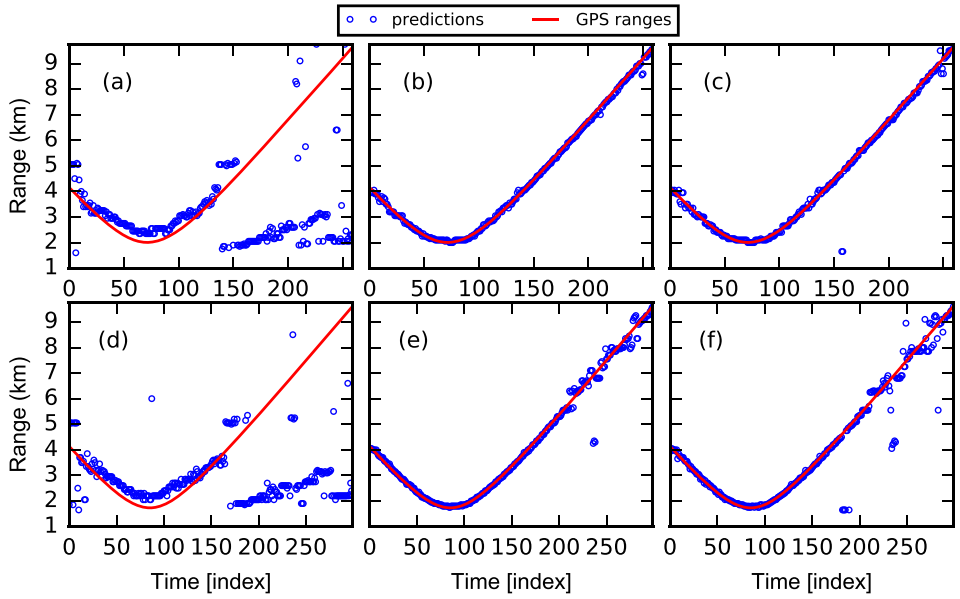

Fig. 3. (Color online) Localization results with frequency band 53–200 Hz by Bartlett MFP (a),(d); SVM classifier (b),(e); and FNN classifier (c),(f). (a)–(c) correspond to Test-Data-1 and (d)–(f) correspond to Test-Data-2. The time index increment is 5 s.

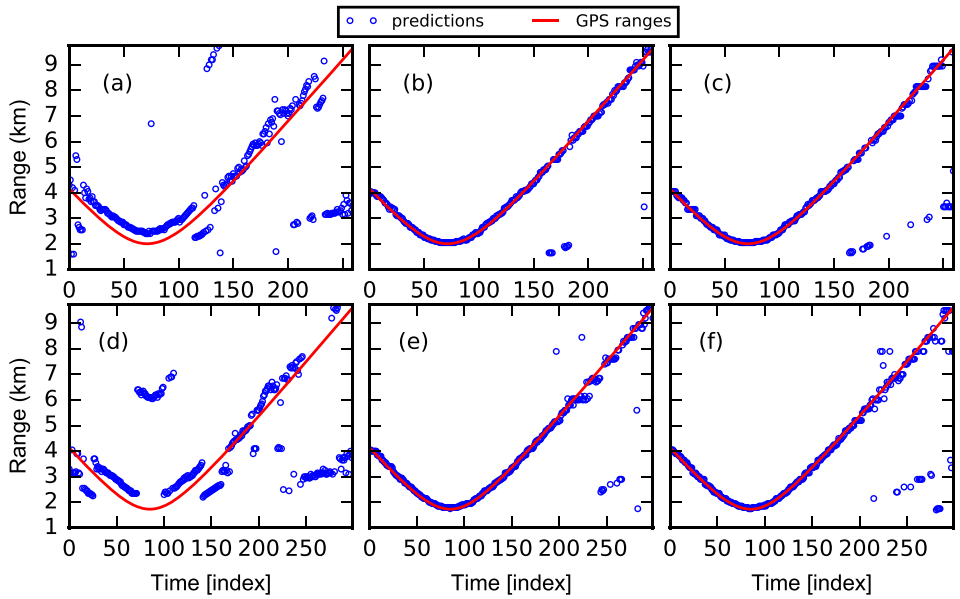

Fig. 4. (Color online) Localization results with frequency band 203–350 Hz by Bartlett MFP (a),(d); SVM classifier (b),(e); and FNN classifier (c),(f). (a)–(c) correspond to Test-Data-1 and (d)–(f) correspond to Test-Data-2. The time index increment is 5 s.

For all cases tested, the SVM has the best performance when evaluated using the MAPE.

This study demonstrates that machine learning classifier methods generate reasonable range predictions without knowledge of the ocean environment, even when the data are from different sources with different moving speeds.

4. Conclusion

In this letter, the Santa Barbara Channel experiment was used to demonstrate the effectiveness of the SVM and FNN machine learning classifiers for acoustic localization using data from different sources of opportunity. The use of training and test data from different ships with different speeds (13–20 kn) indicates that the SVM and FNN localization methods are robust to changes in the source spectrum as suggested in Sec. 2.1 and Ref. 1. Acoustic modeling and estimates of the ship SNR demonstrate that the performance of the conventional MFP, SVM, and FNN degrades at lower SNR (Sec. 3.1). The SVM and FNN classifiers produce reasonable range estimates at long ranges but, with limited environmental information, MFP becomes biased by sidelobes and environmental mismatch at long ranges. As a result, the machine learning classifier methods perform better overall than MFP without detailed environment knowledge (Sec. 3.2).

The SVM and FNN classifier methods are limited by the amount of representative training data available. In the sources of opportunity scenario, this limitation may be overcome in part by the availability of shipping noise from known tracks and AIS data. The effect of large environmental variations on SVM and FNN was not investigated and could include fluctuations in the sound speed profile.

Acknowledgments

This work was supported by the Office of Naval Research under Grant No. N00014–1110439, the China Scholarship Council, and the National Natural Science Foundation of China (Grant Nos. 11434012 and 41561144006).

References and links

[1]H. Niu, E. Reeves, and P. Gerstoft, "Source localization in an ocean waveguide using supervised machine learning," J. Acoust. Soc. Am. **142**, 1176–1188 (2017).
[2]K. L. Gemba, W. S. Hodgkiss, and P. Gerstoft, "Adaptive and compressive matched field processing," J. Acoust. Soc. Am. **141**, 92–103 (2017).
[3]K. L. Gemba, S. Nannuru, P. Gerstoft, and W. S. Hodgkiss, "Multi-frequency sparse Bayesian learning for robust matched field processing," J. Acoust. Soc. Am. **141**, 3411–3420 (2017).
[4]B. Z. Steinberg, M. J. Beran, S. H. Chin, and J. H. Howard, "A neural network approach to source localization," J. Acoust. Soc. Am. **90**, 2081–2090 (1991).
[5]A. Caiti and T. Parisini, "Mapping ocean sediments by RBF networks," IEEE J. Ocean. Eng. **19**, 577–582 (1994).

[6]A. Caiti and S. Jesus, "Acoustic estimation of seafloor parameters: A radial basis functions approach," J. Acoust. Soc. Am. **100**, 1473–1481 (1996).
[7]Y. Stephan, X. Demoulin, and O. Sarzeaud, "Neural direct approaches for geoacoustic inversion," J. Comput. Acoust. **6**, 151–166 (1998).
[8]J. Benson, N. R. Chapman, and A. Antoniou, "Geoacoustic model inversion using artificial neural networks," Inv. Problems **16**, 1627–1639 (2000).
[9]Z. H. Michalopoulou, D. Alexandrou, and C. Moustier, "Application of neural and statistical classifiers to the problem of seafloor characterization," IEEE J. Ocean. Eng. **20**, 190–197 (1995).
[10]R. Lefort, G. Real, and A. Drémeau, "Direct regressions for underwater acoustic source localization in fluctuating oceans," Appl. Acoust. **116**, 303–310 (2017).
[11]C. M. A. Verlinden, J. Sarkar, W. S. Hodgkiss, W. A. Kuperman, and K. G. Sabra, "Passive acoustic source localization using sources of opportunity," J. Acoust. Soc. Am. **138**, EL54–EL59 (2015).
[12]S. H. Byun, C. M. A. Verlinden, and K. G. Sabra, "Blind deconvolution of shipping sources in an ocean waveguide," J. Acoust. Soc. Am. **141**, 797–807 (2017).
[13]Z. Lei, K. Yang, and Y. Ma, "Passive localization in the deep ocean based on cross-correlation function matching," J. Acoust. Soc. Am. **139**, EL196–EL201 (2016).
[14]N. Srivastava, G. E. Hinton, A. Krizhevsky, I. Sutskever, and R. Salakhutdinov, "Dropout: A simple way to prevent neural networks from overfitting," J. Mach. Learn. Res. **15**, 1929–1958 (2014).
[15]M. Abadi, A. Agarwal, P. Barham, E. Brevdo, Z. Chen, C. Citro, G. S. Corrado, A. Davis, J. Dean, M. Devin, S. Ghemawat, I. Goodfellow, A. Harp, G. Irving, M. Isard, Y. Jia, R. Jozefowicz, L. Kaiser, M. Kudlur, J. Levenberg, D. Mane, R. Monga, S. Moore, D. Murray, C. Olah, M. Schuster, J. Shlens, B. Steiner, I. Sutskever, K. Talwar, P. Tucker, V. Vanhoucke, V. Vasudevan, F. Viegas, O. Vinyals, P. Warden, M. Wattenberg, M. Wicke, Y. Yu, and X. Zheng, "TensorFlow: Large-scale machine learning on heterogeneous distributed systems," https://www.tensorflow.org/ (Last viewed July 30, 2017).
[16]D. Kingma and B. Jimmy, "Adam: A method for stochastic optimization," arXiv:1412.6980 (2014).
[17]F. Pedregosa, G. Varoquaux, A. Gramfort, V. Michel, B. Thirion, O. Grisel, M. Blondel, P. Prettenhofer, R. Weiss, V. Dubourg, J. Vanderplas, A. Passos, D. Cournapeau, M. Brucher, M. Perrot, and E. Duchesnay, "Scikit-learn: Machine learning in Python," J. Mach. Learn. Res. **12**, 2825–2830 (2011).
[18]M. B. Porter, "The KRAKEN normal mode program," SACLANT Undersea Research Centre Memorandum (SM-245) and Naval Research Laboratory Memorandum Report No. 6920 (1991).
[19]https://marinetraffic.com (Last viewed July 30, 2017).